Fully differential cross sections for single ionization of helium by energetic protons

I. B. Abdurakhmanov, A. S. Kadyrov, Sh. U. Alladustov, and I. Bray
Curtin Institute for Computation and Department of Physics and Astronomy, Curtin University, GPO Box U1987, Perth, Western Australia 6845, Australia

K. Bartschat
Department of Physics and Astronomy, Drake University, Des Moines, Iowa 50311, USA

(Received 6 October 2019; revised manuscript received 17 November 2019; published 18 December 2019)

Fully differential cross sections for single ionization of helium by fast proton impact in different kinematical regimes in the scattering plane were recently measured in a high-precision experiment [O. Chuluunbaatar *et al.*, Phys. Rev. A **99**, 062711 (2019)] and calculated using the first Born approximation. We use the nonperturbative wave-packet convergent close-coupling approach to calculate this process more accurately in all the kinematical regimes considered in the experiment. The obtained results show that the coupling between channels and multiple-scattering effects, combined with a more accurate treatment of the target structure, significantly improves the agreement between theory and experiment, especially in the apparently most difficult regions away from the so-called Bethe ridge, where the deviation in the positions of the binary peak observed in the experiment and calculated using the first Born approximation is largest. We also present fully differential cross sections in the same kinematical regimes but for incident projectile energies of 500 keV and 2 MeV. Corresponding results for the so-called perpendicular and azimuthal planes are also exhibited.

DOI: 10.1103/PhysRevA.100.062708

I. INTRODUCTION

Studies of fully differential cross sections (FDCSs) play an important role in understanding the dynamics of ion-atom collisions, since these cross sections carry the most detailed information about the collision process. The recently developed reaction microscope known as cold target recoil ion momentum spectroscopy (COLTRIMS) [1], which allows one to measure the three-dimensional momentum distribution of electrons emitted during the collision process in coincidence with the residual ion, has been used to obtain high-precision kinematically complete data [2–6].

There has been considerable progress in the theory of ion-atom collisions as well. A number of theoretical approaches have been developed over the past few decades, which are capable of producing the total ionization cross section in acceptable agreement with experimental measurements over a wide range of impact energies for various collision processes [7–22]. However, when it comes to the FDCS, even the most sophisticated approaches encounter various challenges for certain kinematical regimes.

The worst case is observed for single ionization of helium induced by 100-MeV/amu C^{6+} ion impact when the electron is ejected in the plane perpendicular to the momentum-transfer direction [2]. Most of the existing theoretical models completely fail (with a disagreement of almost a factor of 10) to reproduce the experimental data, both qualitatively and quantitatively (see, e.g., Ref. [23] and references therein). A recent work by Igarashi and Gulyás [24] showed that the convolution of their continuum-distorted-wave–eikonal-initial-state results by the experimental momentum resolution leads to good agreement with the measured FDCS data in this perpendicular plane. Another case is the FDCS for single ionization of helium by 75-keV protons in the perpendicular plane, defined by the initial projectile momentum and the vector normal to the scattering plane, where the available theoretical results are in disagreement with the experiment [3]. Notably, the various theoretical predictions also disagree with each other (see Refs. [25,26] and references therein). This disagreement is more pronounced for higher momentum transfers.

A recent COLTRIMS-based experiment [27] produced ultrahigh-resolution data on the FDCS for single ionization of helium induced by 1-MeV proton impact in 12 different kinematical regimes in terms of momentum transfer and electron ejection energies. The authors stated [6] that their apparatus allowed them to definitely rule out possible experimental sources for disagreement between theory and experiment as they achieved the highest resolution ever reported in such an experiment. Accordingly, the results should serve as an ideal test bed for theoretical calculations.

In addition to presenting their measured data, these authors reported their theoretical calculations obtained using various forms of the first Born approximation (FBA). In particular, they employed the plane-wave FBA, as well as models based on the so-called three-Coulomb (3C) wave function (3C model) and effective charges, including the first-order diagrams with semiclassical postcollision interaction. In their simple FBA approach, both the incident and scattered projectile states were described with plane waves. The 3C model goes somewhat beyond the FBA theory by describing the final asymptotic three-body state with the 3C wave function.

In the model based on effective charges, the authors of [27] studied the effect of varying Sommerfeld parameters of the 3C function on the final results for the FDCS. In this way, a distortion of the intermediate plane waves is achieved.

The model based on semiclassical postcollision interaction investigates the effect of including the postcollisional interaction in the 3C model. As a result of these studies, it was found that the FBA results are reasonable within the Bethe ridge [28], which reaches its maximum when the energy and momentum transfers correspond to the kinematical regime of a free ion-electron collision and can be clearly identified at large momentum-transfer values. The Bethe ridge determines the phase-space region where the FBA gives the largest contributions to the ionization yield, while away from this region one might expect other, higher-order contributions to come into play. This region is given by $q^2/2 = E_e + |\varepsilon_{1s}|$, where q is the momentum transfer of the projectile, E_e is the electron ejection energy, and ε_{1s} is the energy of the active electron in the ground state of helium atom. Beyond that, a combination of the 3C model with a semiclassical postcollision interaction effect improved the agreement with experiment. However, none of the considered models was able to explain the ratio of the recoil- to binary-peak intensity. The 3C model agreed slightly better with experiment in the recoil-peak position, but in the case of the binary peak, a discrepancy of a several degrees with the measured position still remained. It was concluded that all the FBA-like theories have limitations in the kinematical regimes far from the Bethe ridge, even at impact energies as high as 1 MeV. This warrants further investigation of the origin of the disagreement between theory and experiment, employing more sophisticated methods that can couple all possible reaction channels, incorporate multiple-scattering effects, and treat the target structure more accurately by accounting for the electron-electron correlations in the ground and all included states of the two-electron He atom.

In this work we go beyond the perturbative model and apply the wave-packet convergent close-coupling (WP-CCC) approach [22] to study the problem under consideration. When compared to other close-coupling models, a distinct feature of the WP-CCC approach is its ability to generate the target continuum pseudostates with arbitrary ejection energies and the required density in the most relevant region of the spectrum. The energies of the generated continuum pseudostates are aligned across different angular momenta of the target electron, which greatly improves the accuracy of differential ionization studies. Therefore, this approach is ideal for calculating the most detailed fully differential cross sections. At sufficiently high impact energies, where the probability of electron capture is negligible, the method is capable of solving the ionization problems virtually exactly.

II. THE WP-CCC APPROACH

Let us briefly overview the basics of the WP-CCC approach to proton-impact single ionization of helium [22]. We start from the exact four-body Schrödinger equation governing the proton-helium collision system and expand the total scattering wave function in a basis of orthogonal target-centered pseudostates with some unknown coefficients. For the projectile energy of 1 MeV considered in this work, the p-He ionization problem can safely be considered without accounting for the electron-capture channels, as at such high energies the probability of electron transfer is negligible in comparison with the probability of direct scattering and ionization. (For the case when electron capture is important, the two-center WP-CCC approach was recently developed and described in Ref. [29].) After the expansion and the use of a semiclassical approximation, the Schrödinger equation is converted to a set of first-order differential equations for the time-dependent expansion coefficients. This set of equations is solved by the standard Runge-Kutta method.

The basis of orthogonal target-centered pseudostates is formed from the combination of eigenstates describing the active electron of the helium atom and wave-packet pseudostates. Both the eigenstates and the pseudostates are generated numerically. First, following the configuration-interaction approach, the helium wave function is expressed as a linear combination of products of two one-electron orbitals, where one of the helium electrons is confined to the 1s orbital. In this way we ensure that the electron-electron correlations in the target are taken into account in the frozen-core approximation. In the next step, this two-electron wave function is inserted into the Schrödinger equation for the helium target. This converts the target Schrödinger equation into an integro-differential equation for the radial function representing the state of the second electron. For each state of the active electron this integro-differential equation is solved numerically subject to appropriate asymptotic boundary conditions. Some of the radial functions from this set represent continuum states of the active electron. These states are not normalizable and consequently are not suitable for close-coupling calculations. However, this issue can be resolved using the technique described in Refs. [21,22], which uses one-electron radial functions representing continuum states in order to generate normalizable wave packets. All of these wave packets represent nonoverlapping subregions of the continuum and are the integrals of continuum functions over the corresponding subregion. In constructing the wave packets, it is necessary to use the same grid for different angular momenta. This ensures the alignment of the wave-packet pseudostate energies across different angular momenta and greatly simplifies the FDCS calculations.

Our aim here is to investigate whether or not the nonperturbative close-coupling calculations of high-energy proton-impact single ionization of helium yield significant corrections to the first Born calculations, especially for the kinematical regimes beyond the Bethe ridge.

The full scattering amplitude can be calculated from the scattering wave function Ψ_i^+ according to [30,31]

$$T_{fi}(\boldsymbol{k}_f, \boldsymbol{k}_i) = \langle \Phi_f^- | \overleftarrow{H} - E | \Psi_i^+ \rangle, \tag{1}$$

where $\boldsymbol{k}_f$ and $\boldsymbol{k}_i$ are the momenta of the scattered and incident projectile, respectively, Φ_f^- is the asymptotic wave function describing the final state, and the arrow over the four-body Hamiltonian operator H indicates the direction of its action. As discussed in [21], scattering amplitudes for the transitions into bound states of the target are directly defined by the transition amplitudes $T_{fi}^N(\boldsymbol{k}_f, \boldsymbol{k}_i)$, whereas the scattering amplitude for ionization of the active electron with momentum $\boldsymbol{\kappa}$ contains the overlap between the two-electron wave packet $\psi_f^{\rm WP}$ and the active electron's continuum functions φ_f. Accordingly, the ionization amplitude is written as

$$T_{\kappa i}(\boldsymbol{k}_f,\boldsymbol{k}_i) = \langle\varphi_f|\psi_f^{\rm WP}\rangle T_{fi}^N(\boldsymbol{k}_f,\boldsymbol{k}_i) = \sum_{l=0}^{l_{\max}}\sum_{m=-l}^{l}\frac{(-i)^l e^{i\sigma_l}Y_{lm}(\hat{\boldsymbol{\kappa}})T_{nlm\,i}^N(\boldsymbol{k}_f,\boldsymbol{k}_i)}{2\pi\kappa\sqrt{w_n}}, \quad (2)$$

where the index n corresponds to the bin with width w_n, σ_l is the phase of the helium continuum function, and $\kappa=\kappa_n=\sqrt{2\mathcal{E}_n}$, with $\mathcal{E}_n$ the energy of the wave-packet pseudostate $\psi_{nl}^{\rm WP}$. Consequently, both excitation and ionization amplitudes are obtained upon calculation of the transition matrix elements $T_{fi}^N(\boldsymbol{k}_f,\boldsymbol{k}_i)$, which are related to the impact-parameter space transition probability amplitudes $a_f(\infty,\boldsymbol{b})$ through[1]

$$T_{fi}^N(\boldsymbol{k}_f,\boldsymbol{k}_i) = \frac{1}{2\pi}\int d\boldsymbol{b}\,e^{i\boldsymbol{p}_\perp\boldsymbol{b}}[a_f(\infty,\boldsymbol{b})-\delta_{fi}] = e^{im(\varphi_f+\pi/2)}\int_0^\infty db\,b[\tilde{a}_f(\infty,b)-\delta_{fi}]J_m(q_\perp b), \quad (3)$$

where $\boldsymbol{q}=\boldsymbol{k}_i-\boldsymbol{k}_f$, $\tilde{a}_f(t,b)=e^{im\phi_b}a_f(t,\boldsymbol{b})$, and $\boldsymbol{b}$ is the impact parameter.

The FDCS is defined as

$$\frac{d^5\sigma(\boldsymbol{k}_f,\boldsymbol{k}_i,\boldsymbol{\kappa})}{dEd\Omega_e d\Omega_f} = \mu^2\frac{k_f\kappa}{k_i}|T_{\kappa i}(\boldsymbol{k}_f,\boldsymbol{k}_i)|^2. \quad (4)$$

It describes the ionization process when the projectile is scattered into a solid angle $d\Omega_f$ around the direction Ω_f, while the electron of the target is ejected into a solid angle $d\Omega_e$ around the direction Ω_e with energy between E_e and E_e+dE_e in terms of the ionization amplitude. For details regarding the calculation of the ionization amplitude, see Refs. [21,32]. A slightly different definition, in terms of the polar angle θ_e and azimuthal angle ϕ_e instead of the solid angle, reads

$$\frac{d^5\sigma(\boldsymbol{q}_f,\boldsymbol{q}_i,\boldsymbol{\kappa})}{dEd\theta_e d\phi_e d\Omega_f} = |\sin\theta_e|\mu^2\frac{q_f\kappa}{q_i}|T_{\kappa i}(\boldsymbol{q}_f,\boldsymbol{q}_i)|^2. \quad (5)$$

We refer to this definition as the FDCS*. A similar definition is used in Ref. [27]. The authors of [27] note that the FDCS* is informative about the so-called kinks, effects that are difficult to see in the measurement. As mentioned in Ref. [27], they appear due to the asymmetry of the FDCS in the angular regions around the forward and backward directions. However, the main reason for the kinks in the FDCS* appears to be the presence of $|\sin\theta_e|$ that drags the cross section to zero in the forward and backward directions. Therefore, they hardly provide any physical information about the process. Here we use both FDCS* and the traditional definition of FDCS. The FDCS* results are presented on a logarithmic scale as in Ref. [27], whereas the FDCS predictions are presented on a linear scale. The latter scale clearly highlights the deficiencies of the FBA models that are not clearly noticeable on the logarithmic scale.

[1]Since we work with the full interaction potential, the transition probability amplitudes include the heavy-particle interaction.

III. RESULTS

Here we present the WP-CCC results for single ionization of helium by proton impact at 1 MeV at several values of the momentum transfer and energies of electrons ejected in the scattering, perpendicular, and azimuthal planes. The azimuthal plane is defined perpendicular to the incident projectile momentum, while the perpendicular plane is defined by the initial projectile momentum and the vector normal to the scattering plane. We compare our results with the experiment [27] for the corresponding scattering-plane geometries. The electron ejection angle θ_e runs from -180° to 180° relative to the incident direction of the projectile in all considered cases, except for the calculations for the azimuthal plane where the angle ϕ_e runs from -180° to 180° relative to the x axis.

Figure 1 shows our results for the FDCS* in the scattering plane in comparison with the experimental data and the FBA calculations of Chuluunbaatar *et al.* [27] for the ejected-electron energies $E_e = 2.5$, 5, 10, and 20 eV and three projectile scattering angles. The projectile scattering angles are given by the momentum transfer $q = 0.5$, 1, and 1.75 a.u. We see good agreement with experiment at all electron emission angles for every kinematical regime considered here. Furthermore, in comparison with the FBA results, the present calculations show better agreement with experiment in all cases displayed. The largest discrepancy between the present results and the FBA calculations is observed in the kinematical regimes that deviate from the Bethe-ridge region the most. Here the disagreement between the previous theories and experiment was most significant. Thus coupling between the channels and multiple-scattering effects significantly improve the agreement with the experiment.

There are kinks in the FDCS* near the forward and backward directions at $q = 0.5$ a.u. The latter become more pronounced as the ejection energy increases. Interestingly, the simple FBA appears to reproduce them. We note that the FBA results shown in Fig. 1 are convolved with experimental uncertainties in ejected-electron energy and momentum transfer while other two, more sophisticated theories are not. One can see that convolution somewhat fills the depth of the cross section leading to better agreement with the experiment. Such kinks appear also in the WP-CCC calculations, but they do not match the experimental points. It is noteworthy that for the ejected-electron energy of 20 eV and momentum transfer $q = 0.5$ a.u., the more accurate 3C plus Roothaan-Hartree-Fock results of [27], obtained using a model based on the Roothaan-Hartree-Fock approximation for the helium ground state and the 3C wave function for the final channel with inclusion of postcollisional interactions, are in better agreement with our present WP-CCC calculations near the forward and backward directions. The observations made above are easier to see in Fig. 2, which displays the results from Fig. 1 in a more traditional form. The experimental results for the FDCS were obtained from the FDCS* data presented in Ref. [27] by dividing the latter by $|\sin\theta_e|$ and a kinematic factor reflecting the difference between the two definitions of the fully differential cross section.

The present WP-CCC results also yield better agreement with experiment for the positions of the binary and recoil peaks. Our results are fully convergent (within the

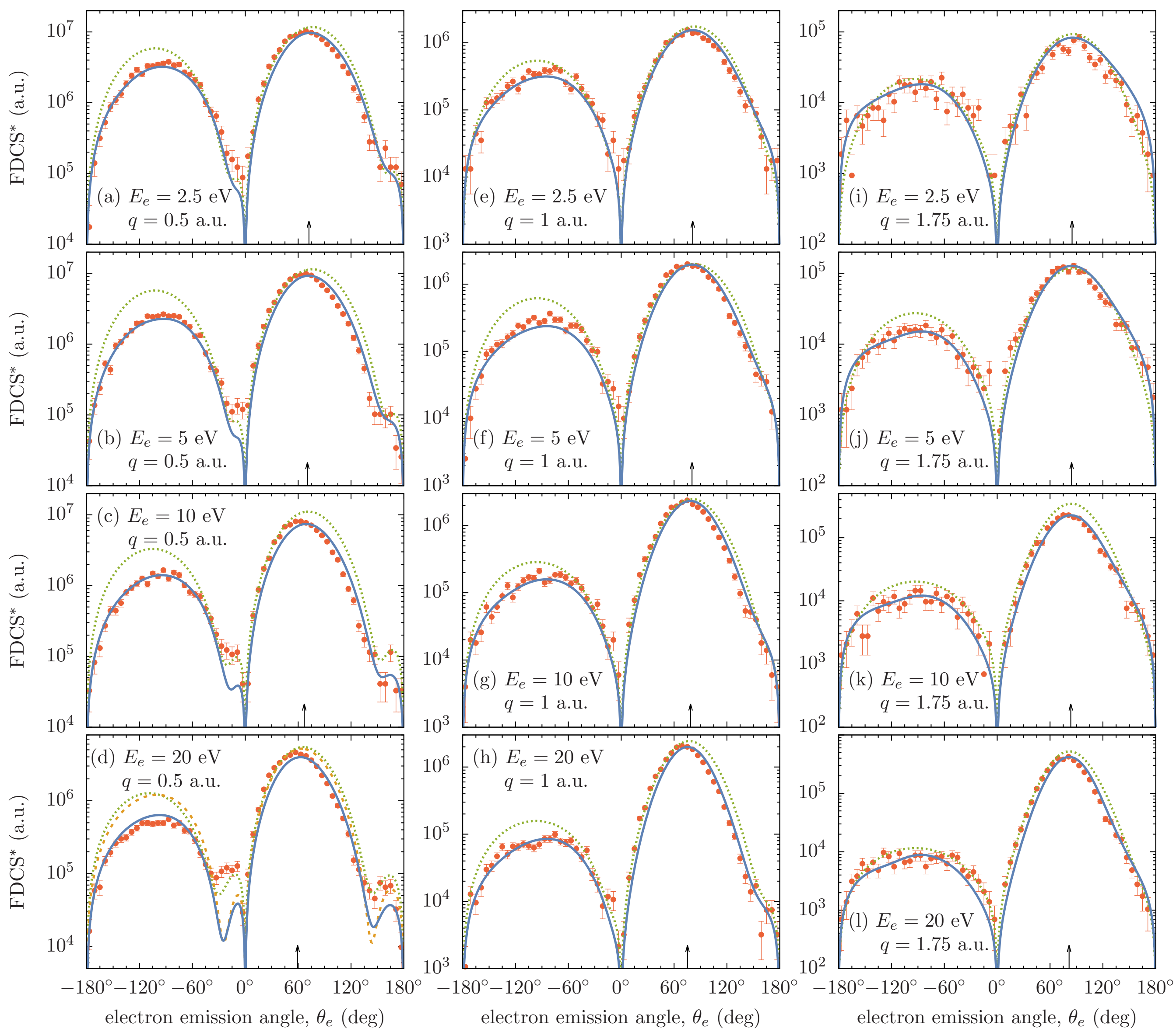

FIG. 1. Fully differential cross sections (FDCS*) for single ionization of helium by 1-MeV protons in the scattering plane ($\phi_e = 0°$) as a function of the polar angle of the ejected electron for the electron emission energies and momentum transfers indicated in the legend. The present WP-CCC predictions (shown by blue solid lines) are compared with the experimental data (red dots with error bars), FBA (green dotted lines), and 3C (brown dashed lines) calculations by Chuluunbaatar *et al.* [27]. The FBA results of Chuluunbaatar *et al.* [27] are convolved with the experimental uncertainties in ejected energy ΔE_e and momentum transfer Δq. The arrow in each panel indicates the direction of the momentum transfer.

frozen-core approximation). Therefore, we believe that the remaining small discrepancy in the peak angles could be due to the frozen-core approximation used. A multicore approach may lead to better agreement with the experiment. Recent studies of the FDCS for this collision system indicate that a better treatment of the helium structure leads to the improved agreement with experiment. For instance, Chuluunbaatar *et al.* [33] obtained good agreement with experiment [6] for the recoil peaks in coplanar kinematics and the binary- to recoil-peak ratio in the case of an accurate, strongly correlated initial function and the 3C final function describing the system before and after the collision. At the same time, we have to mention that the experimental resolution for the considered values of the momentum transfer is reported to be $\Delta q = \pm 0.15$, ± 0.25, and ± 0.4 a.u. for $q = 0.5$, 1.0, and 1.75 a.u., respectively. Hence, the aforementioned discrepancy is very close to the experimental uncertainty.

As mentioned earlier, the displayed FBA results of Chuluunbaatar *et al.* [27] are convolved with experimental uncertainties, whereas our present CCC results are not. Chuluunbaatar *et al.* [27] indicated that the convolution of the calculated data can shift the position of the binary peak towards the experiment. However, the change of the position of their FBA binary peak due to the convolution was found to be small.

Figure 3 presents our predictions for the FDCS in the scattering plane for He single ionization by 0.5- and 2.0-MeV protons, in anticipation of experimental data [34] at these

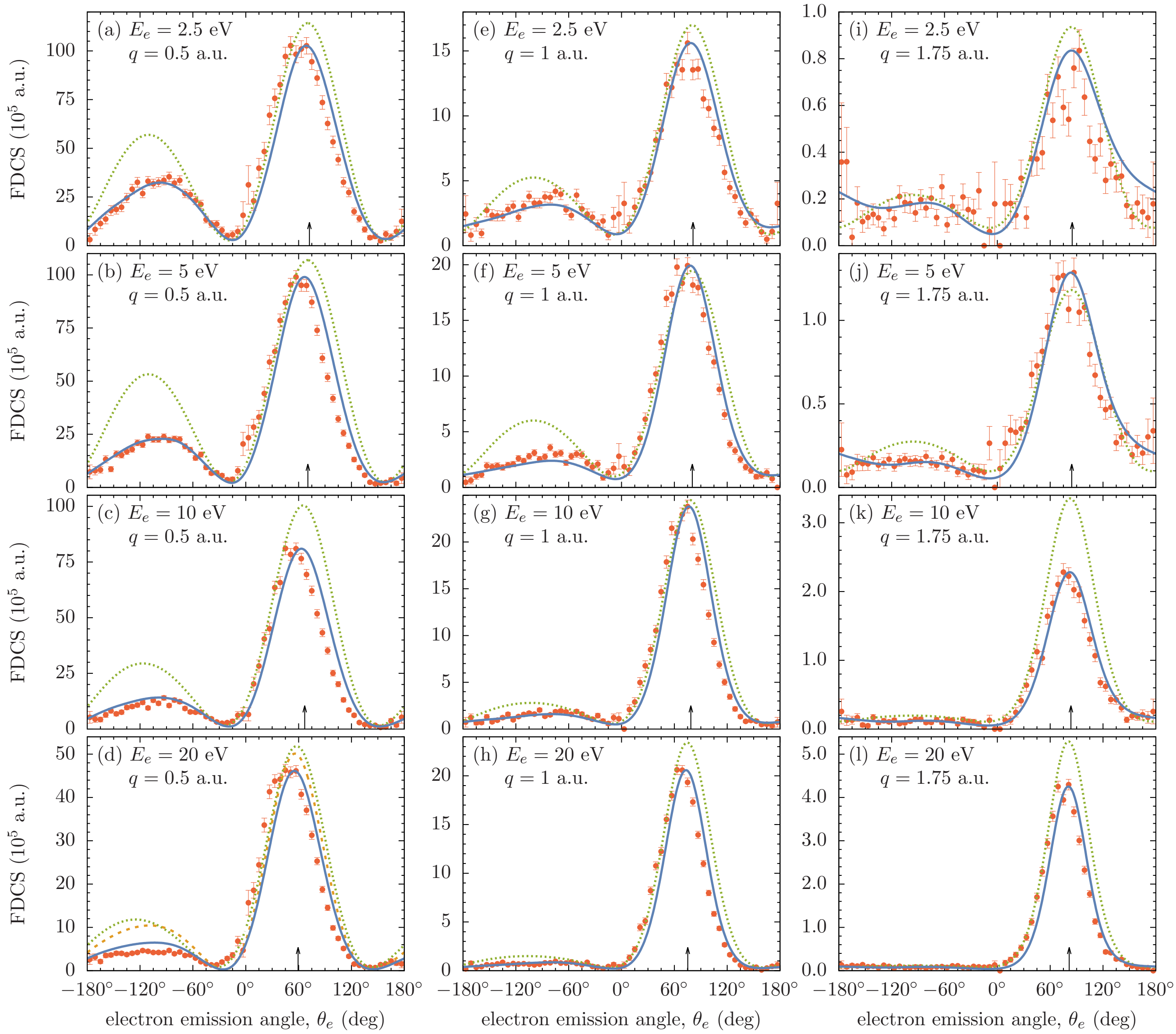

FIG. 2. Fully differential cross sections (FDCS) for single ionization of helium by 1-MeV protons in the scattering plane ($\phi_e = 0^\circ$) as a function of the polar angle of the ejected electron for the electron emission energies and momentum transfers indicated in the legend. The present WP-CCC predictions (shown by blue solid lines) are compared with the experimental data (red dots with error bars), FBA (green dotted lines), and 3C (brown dashed lines) calculations by Chuluunbaatar *et al.* [27]. The FBA results of Chuluunbaatar *et al.* [27] are convolved with the experimental uncertainties in ejected energy ΔE_e and momentum transfer Δq. The arrow in each panel indicates the direction of the momentum transfer.

impact energies. One can see that with increasing projectile energy the position of the binary peak moves towards larger ejection angles. This is due to the change in the direction of the momentum transfer. The latter shifts towards larger angles with increasing projectile energy. For a given momentum transfer, the binary- to recoil-peak ratio reduces as the ejection energy increases. The same happens for a fixed ejection energy as the momentum transfer goes up. As a result, there is no recoil peak at $E_e = 20$ eV and $q = 1.75$ a.u.

Figure 4 shows our predictions for the FDCS in the azimuthal plane. Gassert *et al.* [6] performed FDCS measurements in this plane at 1 MeV for $E_e = 6.5$ eV and $q = 0.75$ a.u. The WP-CCC approach described the experiment [22] well. Here we extend these calculations to 0.5 and 2 MeV and to the kinematical regimes displayed in Figs. 1–3. As the ejection energy and momentum transfer increase, the difference in the FDCS at different collision energies decreases. In addition, here the binary- to recoil-peak ratio decreases again, as the ejection energy and momentum transfer increase, until the recoil peak eventually disappears.

Finally, Fig. 5 exhibits our predictions for the FDCS in the perpendicular plane. This plane corresponds to the one used by Schulz in experiments for single ionization of He by 75-keV protons [3] and 100-MeV/amu C^{6+} ions [2]. Here we

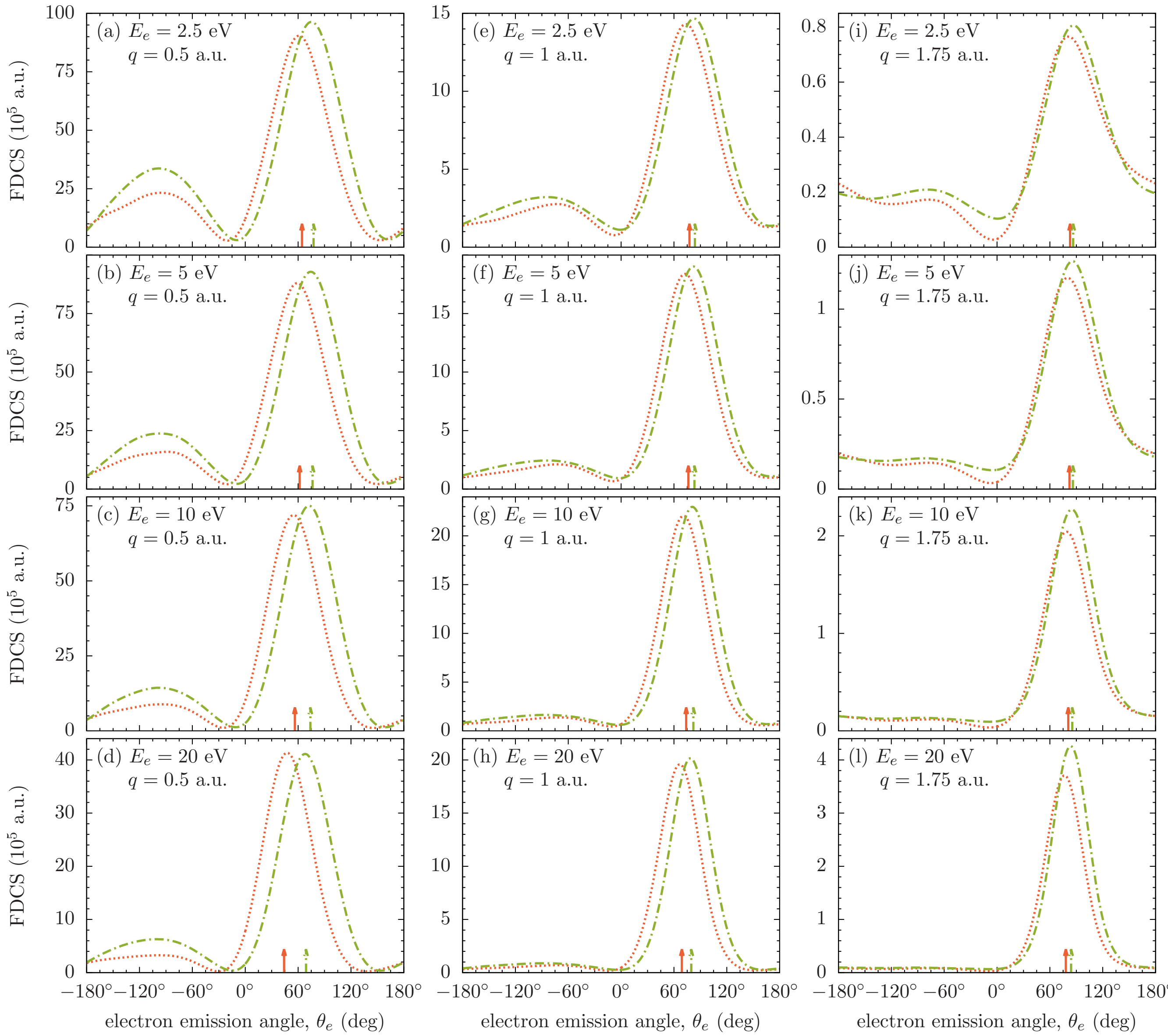

FIG. 3. WP-CCC calculations for the fully differential cross sections for single ionization of helium by 500-keV (red dotted lines) and 2-MeV (green dot-dashed lines) protons in the scattering plane ($\phi_e = 0^\circ$) as a function of the polar angle of the ejected electron for the electron emission energies and momentum transfers indicated in the legend. The arrow in each panel indicates the direction of the momentum transfer.

present calculations for the same kinematical regimes as used in Figs. 1–4. The FDCS in this plane is significantly smaller than the FDCS in the other two planes considered. Notably, we see two peaks, one in the forward direction and the other in the backward direction, in all kinematic regimes considered. This is consistent with our earlier calculations for the C^{6+}-He system. However, according to the measurements by Schulz *et al.* [2], the C^{6+}-He FDCS peaks at $\theta_e = \pm 90^\circ$. Gassert *et al.* [6] attempted to shed light onto this subject by performing the aforementioned experiments with 1-MeV protons in the scattering and azimuthal planes. However, without experiments specifically designed for the perpendicular plane, the question "whether this disagreement between theory and experiment is due to fundamental reasons that indicate a general problem in the field of ion-atom collisions" [6] will remain open.

IV. CONCLUSION

The wave-packet convergent close-coupling method was applied to calculate the fully differential cross section for proton-induced single ionization of the helium ground state at incident projectile energies of 0.5, 1, and 2 MeV in the scattering, perpendicular, and azimuthal planes. Generally very good agreement with recent experimental data was obtained at 1 MeV for all considered kinematical regimes in the scattering plane. The advantage of the present WP-CCC approach results over the FBA-type ones is particularly pronounced for the kinematical regimes that are further away from the Bethe-ridge region. The obtained results show that the coupling between channels and multiple-scattering effects are important and improve the agreement between theory and experiment, especially for the position of the recoil peak.

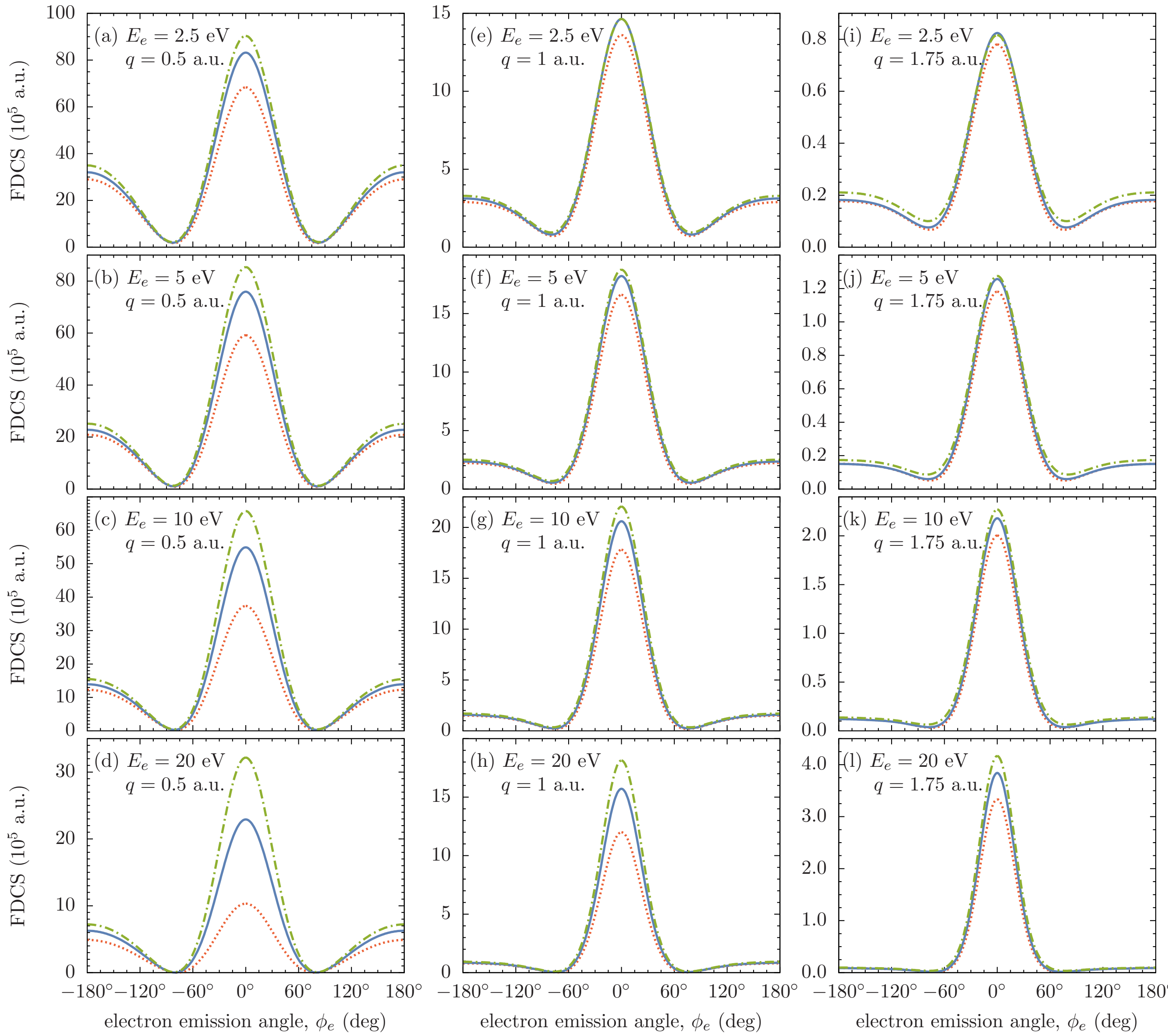

FIG. 4. WP-CCC results for the fully differential cross sections for single ionization of helium by 500-keV (red dotted lines), 1-MeV (blue solid lines), and 2-MeV (green dot-dashed lines) protons in the azimuthal plane ($\theta_e = 90^\circ$) as a function of the azimuthal angle of the ejected electron for the electron emission energies and momentum transfers indicated in the legend.

We neglected channels representing the possible capture of the electron by the projectile. However, it is unlikely that accounting for these channels would significantly change the present results. At high energies the probability of electron capture into the bound states and the continuum of the projectile is negligible. The calculations can be further improved by refining the description of the target structure by allowing core-electron excitations. However, this improvement is not expected to change the physics of the ionization process significantly.

The next challenge is the intermediate energy region, where the disagreement between theory and experiment is substantial. As mentioned earlier, at 75 keV for the FDCS describing the single ionization of helium in the perpendicular plane, qualitative and quantitative discrepancies between experiment [3] and theory remain (see Ref. [26] and references therein). This is the energy region where electron transfer is the dominant channel. Accordingly, the probability of electron capture into the bound states and continuum of the projectile cannot be neglected. The recently developed two-center WP-CCC approach [29] may shed some light onto the situation. We note that calculations of the doubly differential cross sections for proton-impact ionization of hydrogen at 75 keV using the two-center WP-CCC approach [35] gave good agreement with experiment for all ejected-electron energies where data are available. The convergent close-coupling method was also succesfully applied to calculate the FDCS for ionization of helium by electron impact [36] for the full range of kinematics and collision geometries of practical interest, including the out-of-plane geometries.

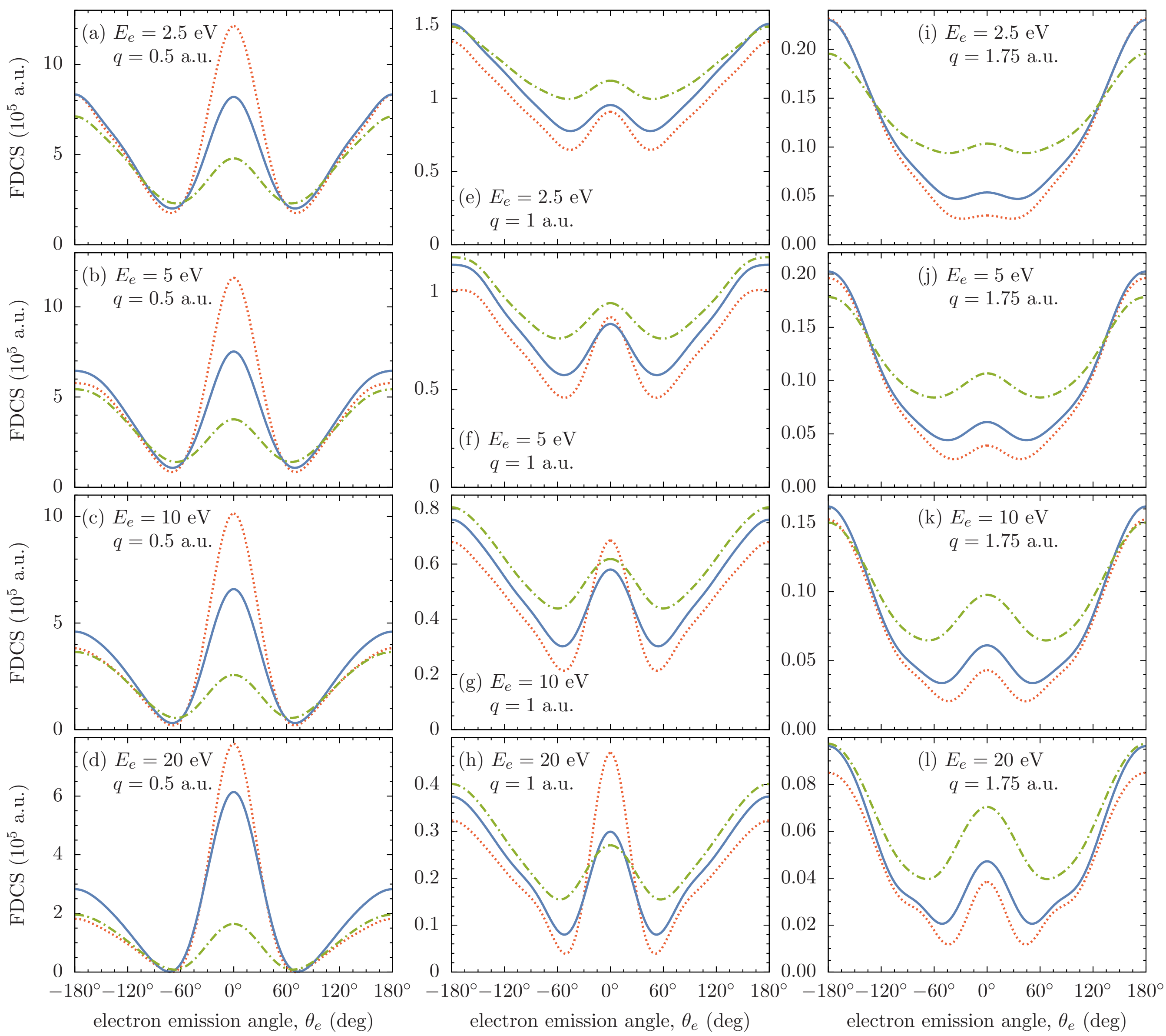

FIG. 5. WP-CCC calculations for the fully differential cross sections for single ionization of helium by 500-keV (red dotted lines), 1-MeV (blue solid lines), and 2-MeV (green dot-dashed lines) protons in the perpendicular plane ($\phi_e = 90^\circ$) as a function of the polar angle of the ejected electron for the electron emission energies and momentum transfers indicated in the legend.

ACKNOWLEDGMENTS

The work was supported by the Australian Research Council. We are grateful for access to the Australian National Computing Infrastructure Facility and the Pawsey Supercomputing Centre in Western Australia. K.B. acknowledges support from the US National Science Foundation under Award No. PHY-1803844. We thank Ochbadrah Chuluunbaatar for providing the experimental and theoretical results of [27] in tabulated form.

[1] J. Ullrich, R. Moshammer, A. Dorn, R. Dörner, L. P. H. Schmidt, and H. Schmidt-Böcking, Rep. Prog. Phys. **66**, 1463 (2003).

[2] M. Schulz, R. Moshammer, D. Fischer, H. Kollmus, D. H. Madison, S. Jones, and J. Ullrich, Nature (London) **422**, 48 (2003).

[3] M. Schulz, A. Hasan, N. V. Maydanyuk, M. Foster, B. Tooke, and D. H. Madison, Phys. Rev. A **73**, 062704 (2006).

[4] A. C. Laforge, K. N. Egodapitiya, J. S. Alexander, A. Hasan, M. F. Ciappina, M. A. Khakoo, and M. Schulz, Phys. Rev. Lett. **103**, 053201 (2009).

[5] M. Schulz, A. C. Laforge, K. N. Egodapitiya, J. S. Alexander, A. Hasan, M. F. Ciappina, A. C. Roy, R. Dey, A. Samolov, and A. L. Godunov, Phys. Rev. A **81**, 052705 (2010).

[6] H. Gassert, O. Chuluunbaatar, M. Waitz, F. Trinter, H.-K. Kim, T. Bauer, A. Laucke, C. Müller, J. Voigtsberger, M. Weller *et al.*, Phys. Rev. Lett. **116**, 073201 (2016).

[7] A. Igarashi, A. Ohsaki, and S. Nakazaki, Phys. Rev. A **62**, 052722 (2000).
[8] G. Schiwietz, U. Wille, R. D. Muiño, P. D. Fainstein, and P. L. Grande, J. Phys. B **29**, 307 (1996).
[9] L. A. Wehrman, A. L. Ford, and J. F. Reading, J. Phys. B **29**, 5831 (1996).
[10] S. Sahoo, S. Mukherjee, and H. Walters, Nucl. Instrum. Methods Phys. Res. Sect. B **233**, 318 (2005).
[11] M. McGovern, D. Assafrão, J. R. Mohallem, C. T. Whelan, and H. R. J. Walters, Phys. Rev. A **79**, 042707 (2009).
[12] M. McGovern, D. Assafrão, J. R. Mohallem, C. T. Whelan, and H. R. J. Walters, Phys. Rev. A **81**, 032708 (2010).
[13] T. G. Lee, H. C. Tseng, and C. D. Lin, Phys. Rev. A **61**, 062713 (2000).
[14] F. Martin and A. Salin, Phys. Rev. A **54**, 3990 (1996).
[15] M. S. Pindzola, T. G. Lee, and J. Colgan, J. Phys. B **44**, 205204 (2011).
[16] M. Foster, J. Colgan, and M. S. Pindzola, Phys. Rev. Lett. **100**, 033201 (2008).
[17] X. Guan and K. Bartschat, Phys. Rev. Lett. **103**, 213201 (2009).
[18] A. Igarashi, A. Ohsaki, and S. Nakazaki, Phys. Rev. A **64**, 042717 (2001).
[19] I. B. Abdurakhmanov, A. S. Kadyrov, I. Bray, and A. T. Stelbovics, J. Phys. B **44**, 075204 (2011).
[20] I. B. Abdurakhmanov, A. S. Kadyrov, D. V. Fursa, and I. Bray, Phys. Rev. Lett. **111**, 173201 (2013).
[21] I. B. Abdurakhmanov, A. S. Kadyrov, and I. Bray, J. Phys. B **49**, 03LT01 (2016).
[22] I. B. Abdurakhmanov, A. S. Kadyrov, I. Bray, and K. Bartschat, Phys. Rev. A **96**, 022702 (2017).
[23] I. B. Abdurakhmanov, I. Bray, D. V. Fursa, A. S. Kadyrov, and A. T. Stelbovics, Phys. Rev. A **86**, 034701 (2012).
[24] A. Igarashi and L. Gulyás, J. Phys. B **52**, 245203 (2019).
[25] M. Dhital, S. Bastola, A. Silvus, B. R. Lamichhane, E. Ali, M. F. Ciappina, R. Lomsadze, A. Hasan, D. H. Madison, and M. Schulz, Phys. Rev. A **100**, 032707 (2019).
[26] X. Niu, S. Sun, F. Wang, and X. Jia, Phys. Rev. A **96**, 022703 (2017).
[27] O. Chuluunbaatar, K. A. Kouzakov, S. A. Zaytsev, A. S. Zaytsev, V. L. Shablov, Y. V. Popov, H. Gassert, M. Waitz, H.-K. Kim, T. Bauer *et al.*, Phys. Rev. A **99**, 062711 (2019).
[28] M. Inokuti, Rev. Mod. Phys. **43**, 297 (1971).
[29] S. U. Alladustov, I. B. Abdurakhmanov, A. S. Kadyrov, I. Bray, and K. Bartschat, Phys. Rev. A **99**, 052706 (2019).
[30] A. S. Kadyrov, I. Bray, A. M. Mukhamedzhanov, and A. T. Stelbovics, Phys. Rev. Lett. **101**, 230405 (2008).
[31] A. S. Kadyrov, I. Bray, A. M. Mukhamedzhanov, and A. T. Stelbovics, Ann. Phys. (NY) **324**, 1516 (2009).
[32] I. B. Abdurakhmanov, A. S. Kadyrov, D. V. Fursa, I. Bray, and A. T. Stelbovics, Phys. Rev. A **84**, 062708 (2011).
[33] O. Chuluunbaatar, S. A. Zaytsev, K. A. Kouzakov, A. Galstyan, V. L. Shablov, and Y. V. Popov, Phys. Rev. A **96**, 042716 (2017).
[34] M. S. Schöffler (private communication).
[35] I. B. Abdurakhmanov, J. J. Bailey, A. S. Kadyrov, and I. Bray, Phys. Rev. A **97**, 032707 (2018).
[36] I. Bray, D. V. Fursa, A. S. Kadyrov, and A. T. Stelbovics, Phys. Rev. A **81**, 062704 (2010).